Springer

Journal of Mechanical Science and Technology 23 (2009) 14~18

Journal of
Mechanical
Science and
Technology

www.springerlink.com/content/1738-494x
DOI 10.1007/s12206-008-1011-7

Compressive characteristics of WBK core depending upon the specimen size †

Byung-Kon Lee, Insu Jeon* and Ki-Ju Kang

Department of Mechanical systems Engineering, Chonnam National University, Gwangju, 500-757, Republic of Korea

(Manuscript Received February 18, 2008; Revised June 14, 2008; Accepted October 15, 2008)

Abstract

Uniaxial compression tests on Wire-woven Bulk Kagome (WBK) specimens of different sizes are carried out to measure their stress-strain behaviors and compressive properties, such as the effective elastic modulus and peak stress. The analytical models for estimating the compressive properties are reviewed and the measured properties are compared with analytically predicted ones. The compressive characteristics depending on the WBK specimen size are finally analyzed through the experimental investigation of the deformed shapes of the different size specimens.

Keywords: Compressive performance; Effective elastic modulus; Peak stress; Specimen size; Wire-woven Bulk Kagome (WBK)

1. Introduction

Periodic cellular metals (PCMs) are lightweight materials classified as pyramidal, lattice block, tetrahedral, metal textile and 3-D Kagome truss cellular metals [1-6]. They have attracted considerable attention due to their excellent specific strength and stiffness, and show great potential for multi-functional applications.

In particular, Hyun et al. [5] demonstrated by using finite element analysis that the Kagome truss PCM shows superior isotropy and stability of plastic deformation under compression as well as shear loading than that of the tetragonal truss. Wang et al. [6] showed the same benefits after fabricating the Kagome truss PCM by investment casting and measuring the compressive performance of sandwich panels with the Kagome core. Lim and Kang [7] introduced two fabrication techniques for single layered truss PCMs based on three-axes weaving, and examined mechanical strengths of sandwich panels with the truss PCM cores.

Recently, Lee et al. [8] devised a new type of PCM named Wire-woven bulk Kagome (WBK), which can be fabricated by systematical assembly using helical metal wires, and which guarantees mass production of robust PCMs with high specific strength.

In this investigation, the stress-strain curves of the WBK specimens of different sizes and their compressive properties, such as the effective elastic modulus and peak stress, have been measured. The analytical models for estimating the compressive properties have been reviewed, and the measured properties have been compared with the analytically predicted ones. Finally, their compressive characteristics depending on the specimen size have been experimentally analyzed. .

2. Prediction of compressive properties

After considering the constraint-free condition for the boundary surface of the WBK specimen under the state of force equilibrium, it is found that only the wires attached to both upper and lower face sheets sustain all the external loads [8]. Therefore, the effective elastic modulus, E_e, can be determined from

† This paper was recommended for publication in revised form by Associate Editor Chongdu Cho

*Corresponding author. Tel.: +82 62 530 1688, Fax.: +82 62 530 1689
E-mail address: i_jeon@chonnam.ac.kr

force equilibrium and elastic energy conservation by using the struts constituting those wires as follows [8]:

$$\sigma_{peak} = \sigma_c \frac{N}{V_e} a \frac{\pi d^2}{6} \quad (1)$$

where, $V_e = L_e \times W_e \times H$ is the effective volume for the WBK core that actually bears the outer loading. Here, L_e is the effective length, W_e is the effective width and H is the height of the WBK core (see Figs. 1(a) and 1(b)). Moreover, N is the total number of load-sustaining struts in the effective volume, a is the length of a strut, E_s and $d = 2r$ are the elastic modulus and diameter of the strut, respectively.

The peak stress, σ_{peak} is then, predicted from the equilibrium of the out-of-plane direction as [8]:

$$\sigma_{peak} = \sigma_c \frac{N}{V_e} a \frac{\pi d^2}{6} \quad (2)$$

where σ_c is the critical stress for the plastic buckling of a strut. If the truss PCM is composed of an elastic-strain hardening material, it can fail by plastic buckling. For this case, σ_c can be determined using the Shanley tangent-modulus buckling formula given as [9]:

$$\sigma_c = \frac{k^2 E_t \pi^2 r^2}{4a^2} \quad (3)$$

where, k represents the buckling mode and is taken as "1" for the frictionless pin-joint assumption used in this research. The tangent-modulus, $E_t = \frac{d\sigma}{d\varepsilon}$, in which σ and ε are the respective true stress and strain, is determined from the plastic hardening behavior in the uniaxial true stress-strain curve of the metal wire.

The modified Ramberg-Osgood model [10] is applied to fit the full range stress-strain curve. Then, the critical stress σ_c is given implicitly by using Eqs. (3) and equations for the model as follows [8]:

$$\left(\frac{\pi r}{2l}\right)^2 = \frac{\sigma_c - \sigma_{0.2}}{E_{0.2}} + \varepsilon_u \left(\frac{\sigma_c - \sigma_{0.2}}{\sigma_u - \sigma_{0.2}}\right)^{1.2} + \varepsilon_{0.2} \quad (4)$$

where, $\sigma_{0.2}$ is the 0.2% offset yield stress, $E_{0.2}$ is the tangent modulus of the stress-strain curve at the 0.2% offset yield stress, ε_u and σ_u are the ultimate strain and stress, respectively.

For prediction of these compressive properties, the unit WBK structure is idealized as the unit 3-D Kagome structure with straight struts (see Fig. 1(c)) to simplify the problem. Moreover, the frictionless pin-jointed condition, which is a well-verified assumption for estimating the compressive properties of PCM truss cores [1], is applied for each brazed node in the WBK core because the helical wire strut has a sufficiently low aspect ratio, r/a.

3. Uniaxial compression tests

Four different sizes of WBK specimens were fabricated by hand through the fabrication process introduced in Lee et al. [8] (see Figs. 2(a) and 2(b)). Table 1 shows the size of the prepared specimens. Wires of diameter, *d=0.78mm* and strut length, *a=8.1mm* were selected for use in the specimens. Three specimens

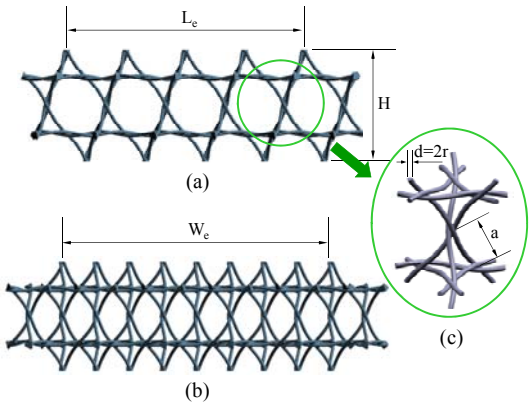

Fig. 1. (a) The effective length L_e and the height H at front view, (b) the effective width W_e at side view, and (c) a unit WBK structure.

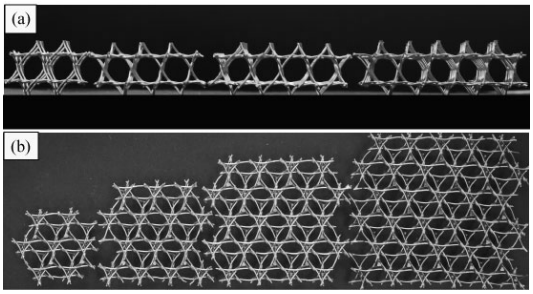

Fig. 2. Different size of WBK specimens: (a) Front view and (b) Top view.

for each specimen size were prepared to check the variations of compression test results. The relative density of the prepared WBK cores, $\bar{\rho}$, equals $\frac{\rho}{\rho_s}$=0.0174. Here, ρ=0.1393g/cm^3 is the density of the WBK core and ρ_s=8g/cm^3 is that of the metal wire, STS304 alloy.

Table 1. The size of prepared specimens.

Relative Density, $\bar{\rho}$	Effective Length, L_e (mm)	Effective Width, W_e (mm)	Height, H (mm)
0.0174	24.3	14.03	27.2
	32.4	28.06	27.2
	48.6	42.09	27.2
	64.8	56.10	27.2

All of the tests were performed on an electric-hydraulic material test system, SATEC TC-55. First, tensile tests for the metal wire were performed in order to obtain the material properties of the annealed wire used for fabricating the WBK cores. From the test results, the 0.2% yield strength, $\sigma_{0.2}$ and effective elastic modulus E_s of STS304 alloy were determined to be $\sigma_{0.2}$=193MPa and E_s=170GPa, respectively. The fitted curve using the modified Ramberg-Osgood model was then obtained from that result [8].

All specimens were loaded up to 20% of the strain to obtain their compressive behaviors. For measuring the effective modulus, an unloading process was carried out before the measured stress reached to the peak stress, and the linear interval in the obtained stress-strain curve under the unloading process was

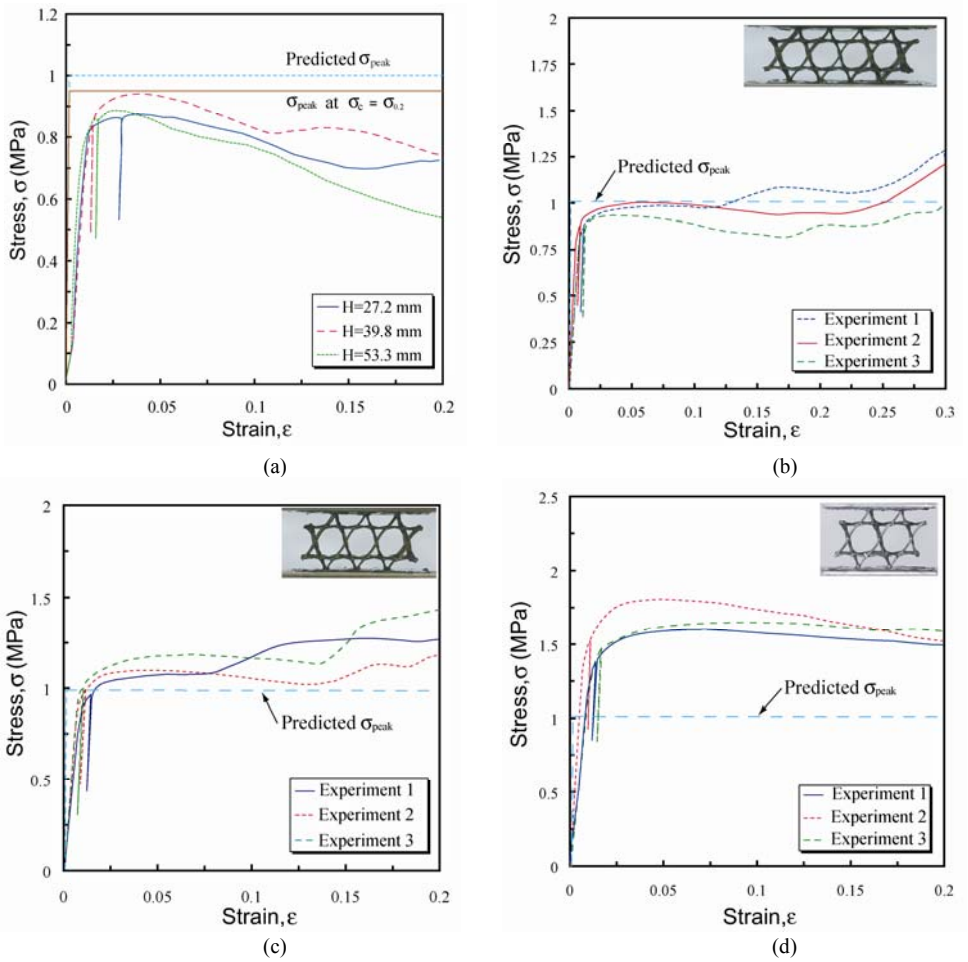

Fig. 3. (a) Representative stress-strain curves of specimens with different heights [8], and measured curves of the specimen with (b) L_e=48.6mm, (c) L_e= 32.4mm and (d) L_e=24.3mm plotted together with the analytically predicted peak stress.

used. Also, the machine compliance, which represents the relation between the displacement of the testing machine and the applied loading, was considered in order to obtain precise specimen displacements [11].

4. Results and discussion

Figs. 3(a)-(d) show the experimentally measured stress-strain curves depending upon the specimen size. In particular, Fig. 3(a) shows the results of Lee et al. [8], which are introduced for comparison with the results of this research. Fig. 3(a) shows the representative stress-strain curve of specimens of same L_e=64.8mm and W_e=56.1mm but different heights, H=27.2, 39.8 and 53.3mm. Figs. 3(b)-(d) show the stress-strain curves of specimens of the same H=27.2mm but different values of L_e and W_e, which are presented in Table 1. The analytically predicted peak stresses calculated by using Eq. (2) were plot ted together in all figures.

Consistent stress-stain behaviors with small variations were obtained in each size of specimen. From the curves in Figs. 3(b)-(d), the effective moduli and peak stresses of each specimen were measured and tabulated in Tables 2 and 3 together with their analytically predicted ones. Tables 2 and 3 demonstrate the differences between the measured values and predicted values.

Table 2. Measured and predicted effective elastic modulus.

Effective length, L_e (mm)	Exp. No.	Measured elastic modulus, E_e (MPa)	Predicted elastic modulus, E_e (MPa)	Average difference (%)
24.3	1	316.6	585.2	-37.13
	2	506.3		
	3	280.8		
32.4	1	408.1	535	-21.6
	2	430.6		
	3	419.3		
48.6	1	433.9	559	-22.77
	2	454.2		
	3	406.9		

Table 3. Measured and predicted peak stresses.

Effective length, L_e (mm)	Exp. No.	Measured peak stress, σ_{peak} (MPa)	Predicted peak stress, σ_{peak} (MPa)	Average difference (%)
24.3	1	1.6	1.05	+60.27
	2	1.81		
	3	1.64		
32.4	1	1.09	0.96	+16.63
	2	1.09		
	3	1.18		
48.6	1	0.97	1.01	-4.62
	2	0.99		
	3	0.93		

In Table 2, the measured effective moduli of the specimen with L_e=24.3mm shows 37.13% decreased average value than the predicted one. Actually, this difference is similar to the differences of the measured effective moduli presented by Lee et al. [8], which were 31.06% average difference of the specimens with H=53.3mm, 45.6% of the specimens with H=39.8mm and 34.72% of the specimens with H=27.2%. This means that the effective moduli of the specimen are insensitive to the size of the specimen. The large differences between the measured and predicted effective moduli values are believed to arise from the geometric defects of the WBK specimens, which are presently made by hand, and the application of the epoxy used to attach the face sheets to the WBK core. To simplify the process of fabricating the WBK specimens, we used epoxy as an adhesive instead of the metal brazing. The epoxy, however, does not give an exact elastic recovery of the core during the unloading process. Therefore, these differences can be dramatically decreased if the face sheets are brazed with the cores by using the metal paste and the entire fabrication process is automated.

In Table 3, the peak stresses of the specimens with L_e=32.4mm and L_e=24.3mm show increased average values of 16.63% and 60.27%, respectively, over the predicted values. These differences are considerably larger than those of the measured peak stresses presented by Lee et al. [8], which showed a 6.3% average difference of the specimens with H=53.3mm, 2.1% of the specimens with H=39.8mm and 6.3% of the specimens with H=27.2mm. This means that the size of the specimen strongly affects the peak stress. The reason behind these increased peak stresses depending on the specimen size is thought to be due to the boundary effect of the specimen.

Fig. 4 shows the representative struts on the boundary of the WBK cores (see the circled regions). These struts, actually, do not have serious effects on the peak stress of the WBK specimen when the specimen size is large because the struts constituting the wires attached to both upper and lower face sheets mainly carry the external loads. However, if the specimen size

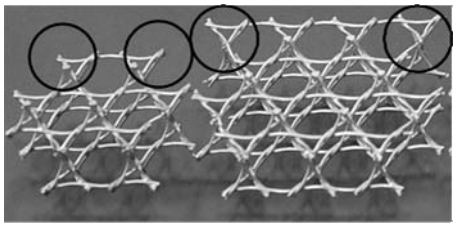

Fig. 4. The struts on the boundary of WBK cores.

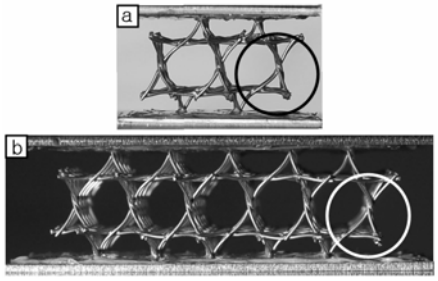

Fig. 5. Deformed shapes under compression of the specimen of (a) L_e= 24.3mm and (b) L_e=64.8 mm.

is decreased, the proportion of the struts on the boundary to the struts constituting the load-carrying wires increases rapidly. Therefore, the effect of the struts on the boundary on the peak stress increases rapidly according to the decrease of the specimen size.

Figs. 5(a) and 5(b) show the deformed shapes of two specimens of different sizes with L_e=24.3mm and L_e=64.8 mm at the peak stress. It is clearly shown that the struts on the boundary of the small specimen are considerably deformed to resist the deformation of the specimen more than the struts of the large one (see the circled regions).

5. Conclusion

The compressive behavior of WBK specimens of different sizes as well as their compressive properties, such as the effective moduli and peak stresses, was measured. Subsequently, the obtained values were compared with analytically predicted ones.

The results show that the effective modulus of the specimen is insensitive to the specimen size but the peak stress of the specimen rapidly increases following the decrease of the specimen size. The reason for this phenomenon is experimentally demonstrated in this research as follows. The proportion of the struts on the boundary to the struts constituting the load-carrying wires increases rapidly following the decrease of the specimen size. Thus, the struts on the boundary of the small specimen strongly resist the deformation of the specimen. This results in the increased peak stresses of the small specimens as compared to the larger ones.

Acknowledgement

This study was supported by National Research Lab program of the Korea Science & Engineering Foundation (R0A-2006-000-10249-0).

References

[1] V. S. Deshpande, N. A. Fleck and M. F. Ashby, Effective Properties of the octet-truss lattice material, *J. Mech. Phys. Solids*, 49 (2001) 1747-1769.

[2] S. Chiras et al., The structural performance of near-optimized truss core panels, *Int. J. Solid. Sturct.*, 39 (2002) 4093-4115.

[3] M. Zupan, V. S. Deshpande and N. A. Fleck, The out-of-plane compressive behaviour of woven-core sandwich plates, *Euro. J. Mech. A/Solids*, 23 (2004) 411-421.

[4] D. T. Queheillalt and H. N. G. Wadley, Pyramidal lattice truss structures with hollow trusses, *Mater. Sci. Eng. A*, 397 (2005) 132-137.

[5] S. Hyun, A. M. Karlsson, S. Torquato and A. G. Evans, Simulated Properties of Kagome and Tetragonal Truss Core Panel, *Int. J. Solid. Struct.*, 40 (2003) 6989-6998.

[6] J. Wang, A. G. Evans, K. Dharmasena and H. N. G. Wadley, On the performance of truss panels with Kagomé cores, *Int. J. Solid. Struct.*, 40 (2003) 6981-6988.

[7] J. H. Lim and K. J. Kang, Mechanical behavior of sandwich panels with tetrahedral and Kagome truss cores fabricated from wires, *Int. J. Solid. Struct.*, 43 (2006) 5228-5246.

[8] Y. H. Lee, B. K. Lee., I. Jeon and K. J. Kang, Wire-Woven Bulk Kagome (WBK) truss cores, *Acta Mater.*, 55 (2007) 6084-6094.

[9] F. R. Shanley, *Mechanics of Materials*, McGraw-Hill, New York, USA, (1967).

[10] K. J. R. Rasmussen, Full-range stress-strain curves for stainless steel alloys, *J. of Constr. Steel Res.*, 59 (2003) 47-61.

[11] I. Jeon and T. Asahina, The effect of structural defects on the compressive behavior of closed-cell Al foam, *Acta Mater.*, 53 (2005) 3415-3423.